YNU-HEPTh-00-101
KUCP-156
May 2000

Parton Distributions in the Virtual Photon Target and Factorization Scheme Dependence*

Ken Sasaki[a] and Tsuneo Uematsu[b]

[a]Department of Physics, Faculty of Engineering, Yokohama National University
Yokohama 240-8501, Japan

[b]Department of Fundamental Sciences, FIHS, Kyoto University,
Kyoto 606-8501, Japan

We investigate parton distributions in the virtual photon target, both polarized and unpolarized, up to the next-leading order (NLO) in QCD. Parton distributions can be predicted completely up to NLO, but they are factorization-scheme-dependent. We analyze parton distributions in several factorization schemes and discuss their scheme dependence. Particular attentions are paid to the axial anomaly effect on the first moments of the polarized quark parton distributions, and also to the large-x behaviors of polarized and unpolarized parton distributions.

1. INTRODUCTION

In e^+e^- collision experiments, we can measure the spin-independent and spin-dependent structure functions, $F_2^\gamma(x,Q^2,P^2)$ and $g_1^\gamma(x,Q^2,P^2)$, of the virtual photon (Fig.1).

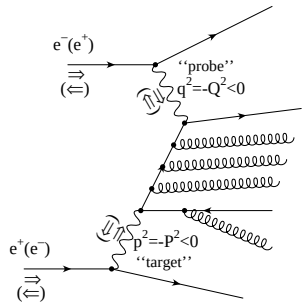

Figure 1. Deep inelastic scattering on a virtual photon in e^+e^- collision.

The advantage in studying the virtual photon target is that, in the case

$$\Lambda^2 \ll P^2 \ll Q^2 \tag{1}$$

where $-Q^2$ $(-P^2)$ is the mass squared of the probe (target) photon, and Λ is the QCD scale parameter, we can calculate the whole structure function up to the next-to-leading order (NLO) by the perturbative method, in contrast to the case of the real photon target where in NLO there exist non-perturbative pieces. The NLO analyses of the virtual photon structure functions, F_2^γ and g_1^γ, have been made by Uematsu and Walsh [1] and the present authors [2], respectively. In this talk we will report the result of our investigation of the parton distribution functions (pdf's) in the virtual photon target. The behaviors of the pdf's can be predicted entirely up to NLO, but they are factorization-scheme-dependent. We carry out our analysis for the pdf's of polarized and unpolarized virtual photon in several different factorization schemes, and see how the pdf's change in each scheme.

2. PARTON DISTRIBUTIONS IN VIRTUAL PHOTON

We write down below the expressions for the polarized case. The expressions for the unpolarized case are easily obtained from the corresponding ones in the polarized case by removing the symble Δ and replacing g_1^γ with F_2^γ/x.

*Talk given by K. Sasaki at the Workshop "Loops and Legs in Quantum Field Theory", Germany, April 2000

Let $\Delta q_S^\gamma(\Delta q_{NS}^\gamma)$, ΔG^γ, $\Delta\Gamma^\gamma$ be the flavor singlet (non-singlet)-quark, gluon, and photon distribution functions, respectively, in the longitudinally polarized virtual photon with mass $-P^2$. In the leading order of the electromagnetic coupling constant, $\alpha = e^2/4\pi$, $\Delta\Gamma^\gamma$ does not evolve with Q^2 and is set to be $\Delta\Gamma^\gamma = \delta(1-x)$. In terms of the Mellin moments of these pdf's, the moment of the polarized virtual photon structure function $g_1^\gamma(x,Q^2,P^2)$ is expressed in the QCD improved parton model as

$$g_1^\gamma(n,Q^2,P^2) = \Delta\boldsymbol{C}^\gamma(n,Q^2)\cdot\Delta\boldsymbol{q}^\gamma(n,Q^2,P^2) \quad (2)$$

where

$$\Delta\boldsymbol{C}^\gamma(n,Q^2) = (\Delta C_S^\gamma\ ,\ \Delta C_G^\gamma\ ,\ \Delta C_{NS}^\gamma\ ,\ \Delta C_\gamma^\gamma)$$
$$\Delta\boldsymbol{q}^\gamma(n,Q^2,P^2) = (\Delta q_S^\gamma\ ,\ \Delta G^\gamma\ ,\ \Delta q_{NS}^\gamma\ ,\ \Delta\Gamma^\gamma)$$

and $\Delta C_S^\gamma(\Delta C_{NS}^\gamma)$, ΔC_G^γ, and ΔC_γ^γ are the moments of the coefficient functions corresponding to singlet(non-singlet)-quark, gluon, and photon, respectively, and they are independent of P^2.

The pdf's $\Delta\boldsymbol{q}^\gamma$ satisfy inhomogeneous evolution equations. The explicit expressions of Δq_S^γ, ΔG^γ, and Δq_{NS}^γ up to the NLO are derived from Eq.(4.46) of Ref.[2]. They are given in terms of one-(two-) loop hadronic anomalous dimensions $\Delta\gamma_{ij}^{(0),n}$ $(\Delta\gamma_{ij}^{(1),n})$ $(i,j=\psi,G)$ and $\Delta\gamma_{NS}^{(0),n}$ $(\Delta\gamma_{NS}^{(1),n})$, one-(two-) loop anomalous dimensions $\Delta K_i^{(0),n}$ $(\Delta K_i^{(1),n})$ $(i=\psi,G,NS)$ which represent the mixing between photon and three hadronic operators R_i^n $(i=\psi,G,NS)$, and finally ΔA_i^n, the one-loop photon matrix elements of these hadronic operators renormalized at $\mu^2 = P^2(=-p^2)$,

$$\langle\gamma(p)\mid R_i^n(\mu)\mid\gamma(p)\rangle|_{\mu^2=P^2} = \frac{\alpha}{4\pi}\Delta A_i^n\ . \quad (3)$$

3. FACTORIZATION SCHEMES

Although g_1^γ is a physical quantity and thus unique, there remains a freedom in the factorization of g_1^γ into $\Delta\boldsymbol{C}^\gamma$ and $\Delta\boldsymbol{q}^\gamma$. Given the formula Eq.(2), we can always redefine $\Delta\boldsymbol{C}^\gamma$ and $\Delta\boldsymbol{q}^\gamma$ as follows [3]:

$$\Delta\boldsymbol{C}^\gamma(n,Q^2) \rightarrow \Delta\boldsymbol{C}^\gamma(n,Q^2)|_a \equiv \Delta\boldsymbol{C}^\gamma(n,Q^2)Z_a^{-1}(n,Q^2)$$
$$\Delta\boldsymbol{q}^\gamma(n,Q^2,P^2) \rightarrow \Delta\boldsymbol{q}(n,Q^2,P^2)|_a \equiv Z_a(n,Q^2)\ \Delta\boldsymbol{q}^\gamma(n,Q^2,P^2)$$

where $\Delta\boldsymbol{C}^\gamma|_a$ and $\Delta\boldsymbol{q}|_a$ correspond to the quantities in a new factorization scheme-a. The most general form of a transformation for the coefficient functions in one-loop order, from $\overline{\rm MS}$ scheme to a new factorization scheme-a, is given by

$$\begin{aligned}
\Delta C_{S,\ a}^{\gamma,\ n} &= \Delta C_{S,\ \overline{\rm MS}}^{\gamma,\ n} - \langle e^2\rangle\frac{\alpha_s}{2\pi}\ \Delta w_a(n)\\
\Delta C_{G,\ a}^{\gamma,\ n} &= \Delta C_{G,\ \overline{\rm MS}}^{\gamma,\ n} - \langle e^2\rangle\frac{\alpha_s}{2\pi}\ \Delta z_a(n)\\
\Delta C_{NS,\ a}^{\gamma,\ n} &= \Delta C_{NS,\ \overline{\rm MS}}^{\gamma,\ n} - \frac{\alpha_s}{2\pi}\ \Delta w_a(n) \qquad (4)\\
\Delta C_{\gamma,\ a}^{\gamma,\ n} &= \Delta C_{\gamma,\ \overline{\rm MS}}^{\gamma,\ n} - \frac{\alpha}{\pi}\ 3\langle e^4\rangle\Delta\hat{z}_a(n)
\end{aligned}$$

where $\langle e^2\rangle = \sum_i e_i^2/N_f$, $\langle e^4\rangle = \sum_i e_i^4/N_f$, with N_f being the number of flavors of active quarks and e_i being the electric charge of i-flavor-quark.

Once the relations (4) between the coefficient functions in the a-scheme and $\overline{\rm MS}$ scheme are given, we can derive corresponding transformation rules [4] from $\overline{\rm MS}$ scheme to a-scheme for the relevant two-loop anomalous dimensions and also for the one-loop photon matrix elements, ΔA_ψ^n and ΔA_{NS}^n, of the quark operators. Note that, in one-loop order, the photon matrix elements of gluonic operators R_G^n vanish in any scheme, $\Delta A_G^n = 0$.

We consider three different factorization schemes both in the polarized and unpolarized cases.

3.1. The polarized case

(i) [The $\overline{\rm MS}$ scheme] This is the only scheme in which both relevant one-loop coefficient functions and two-loop anomalous dimensions [5, 6] were actually calculated. In the $\overline{\rm MS}$ scheme, the QCD (QED) axial anomaly resides in the quark distributions and not in the gluon (photon) coefficient function[7, 8]. In fact we observe

$$\begin{aligned}
\Delta\gamma_{\psi\psi,\ \overline{\rm MS}}^{(1),n=1} &= 24C_FT_f \neq 0\ ,\\
\Delta B_{G,\ \overline{\rm MS}}^{n=1} &= \Delta B_{\gamma,\ \overline{\rm MS}}^{n=1} = 0\ . \qquad (5)
\end{aligned}$$

Also the first moment of the one-loop photon matrix element of quark operators gains the non-zero

values, i.e.,

$$\Delta A^{n=1}_{\psi,\ \overline{\rm MS}} = \frac{\langle e^2\rangle}{\langle e^4\rangle - \langle e^2\rangle^2}\ \Delta A^{n=1}_{NS,\ \overline{\rm MS}} = -12\langle e^2\rangle N_f \quad (6)$$

which is due to the QED axial anomaly.

(ii) [The chirally invariant (CI) scheme] In this scheme the factorization of the photon-gluon (photon-photon) cross section into the hard and soft parts is made so that chiral symmetry is respected and all the anomaly effects are absorbed into the gluon (photon) coefficient function[8, 9]. Thus the spin-dependent quark distributions in the CI scheme are anomaly-free. In particular, we have

$$\Delta B^{n=1}_{G,\ \rm CI} = -2N_f\ , \quad \Delta B^{n=1}_{\gamma,\ \rm CI} = -4 \quad (7)$$
$$\Delta\gamma^{(1),n=1}_{\psi\psi,\ \rm CI} = 0\ , \quad \Delta A^{n=1}_{\psi,\ \rm CI} = \Delta A^{n=1}_{NS,\ \rm CI} = 0\ .$$

The transformation from the $\overline{\rm MS}$ scheme to the CI scheme is achieved by

$$\Delta w_{\rm CI}(n) = 0\ ,$$
$$\Delta z_{\rm CI}(n) = \Delta\hat{z}_{\rm CI}(n) = 2N_f\frac{1}{n(n+1)}\ . \quad (8)$$

(iii) [The off-shell (OS) scheme] In this scheme [10] we renormalize operators while keeping the incoming particle off-shell, $p^2 \neq 0$, so that at renormalization (factorization) point $\mu^2 = -p^2$, the finite terms vanish. This is exactly the same as "the momentum subtraction scheme" which was used some time ago to calculate, for instance, the polarized quark and gluon coefficient functions [11, 12]. The CI-relations in Eq.(7) also hold in the OS scheme. The transformation from $\overline{\rm MS}$ to the OS scheme is made by choosing

$$\Delta w_{\rm OS}(n) = C_F\left\{\Big[S_1(n)\Big]^2 + 3S_2(n) - S_1(n)\Big(\frac{1}{n} - \frac{1}{(n+1)}\Big) - \frac{7}{2} + \frac{2}{n} - \frac{3}{n+1} - \frac{1}{n^2} + \frac{2}{(n+1)^2}\right\} \quad (9)$$
$$\Delta z_{\rm OS}(n) = \Delta\hat{z}_{\rm OS}(n) = N_f\left\{-\frac{n-1}{n(n+1)}S_1(n) + \frac{1}{n} + \frac{1}{n^2} - \frac{4}{(n+1)^2}\right\}\ .$$

It is noted that in the OS scheme we have $\Delta A^n_{\psi,\ \rm OS} = \Delta A^n_{NS,\ \rm OS} = 0$ for all n.

3.2. The unpolarized case

To study the pdf's inside unpolarized virtual photon, we consider three factorization schemes: (i) The $\overline{\rm MS}$ scheme; (ii) The off-shell (OS) scheme; and (iii) The DIS$_\gamma$ scheme. The transformation from $\overline{\rm MS}$ to the OS scheme is achieved by

$$w_{\rm OS}(n) = \Delta w_{\rm OS}(n)$$
$$z_{\rm OS}(n) = \hat{z}_{\rm OS}(n) = N_f\left\{-\frac{n^2+n+2}{n(n+1)(n+2)}S_1(n) + \frac{1}{n} - \frac{1}{n^2} + \frac{4}{(n+1)^2} - \frac{4}{(n+2)^2}\right\}\ . \quad (10)$$

The DIS$_\gamma$ was introduced [13] some time ago for the analysis of the unpolarized real photon structure function $F_2^\gamma(x,Q^2)$ in NLO. In this scheme the direct-photon contribution to F_2^γ is absorbed into the photonic quark distributions, so that we take

$$w_{\rm DIS_\gamma}(n) = z_{\rm DIS_\gamma}(n) = 0$$
$$\hat{z}_{\rm DIS_\gamma}(n) = \frac{N_f}{4}B^n_{\gamma,\ \overline{\rm MS}} \quad (11)$$
$$= N_f\left\{-\frac{n^2+n+2}{n(n+1)(n+2)}S_1(n) - \frac{1}{n} + \frac{1}{n^2} + \frac{6}{n+1} - \frac{6}{n+2}\right\}$$

With these preparations, we now examine the factorization scheme dependence of the pdf's in virtual photon.

4. THE $n = 1$ MOMENTS OF POLARIZED PDF'S

The first moments of polarized pdf's are particularly interesting due to their relevance to the axial anomaly [12]. ¿From now on we omit to write the explicit Q^2- and P^2-dependeces in Δq^γ_S, Δq^γ_{NS}, ΔG^γ and in their unpolarized counterparts. For the CI and OS factorization schemes, we have

$$\Delta w_a(n=1) = 0,$$
$$\Delta z_a(n=1) = \Delta\hat{z}_a(n=1) = N_f \quad (12)$$

where $a = {\rm CI, OS}$. These schemes, therefore, give the same first moments for the pdf's. In fact, we

find $\Delta A^{n=1}_{\psi,\ a} = \Delta A^{n=1}_{NS,\ a} = 0$ and this leads to

$$\Delta q^\gamma_S(n=1)|_a = \Delta q^\gamma_{NS}(n=1)|_a = 0 \tag{13}$$

up to NLO. In these schemes, the axial anomaly effects are transfered to the gluon and photon coefficient functions. On the other hand, in the $\overline{\rm MS}$ scheme the axial anomaly effects are retained in the quark distributions. In fact we obtain for singlet quark pdf, for example,

$$\begin{aligned}&\Delta q^\gamma_S(n=1)|_{\overline{\rm MS}}\\ &= \Big[-\frac{\alpha}{\pi}\ 3\langle e^2\rangle N_f\Big]\\ &\quad\times\left\{1-\frac{2}{\beta_0}\frac{\alpha_s(P^2)-\alpha_s(Q^2)}{\pi}N_f\right\}\ .\end{aligned} \tag{14}$$

The factor $\Big[-\frac{\alpha}{\pi}\ 3\langle e^2\rangle N_f\Big]$ is related to the QED axial anomaly and the term $\frac{2}{\beta_0}\frac{\alpha_s(P^2)-\alpha_s(Q^2)}{\pi}N_f$ is coming from the QCD axial anomaly [14].

For gluon distribution, we obtain in NLO

$$\begin{aligned}&\Delta G^\gamma(n=1)\\ &= \frac{12\alpha}{\pi\beta_0}\langle e^2\rangle N_f\ \frac{\alpha_s(Q^2)-\alpha_s(P^2)}{\alpha_s(Q^2)}\ ,\end{aligned} \tag{15}$$

the same result for $\overline{\rm MS}$, CI and OS schemes.

5. The PDF'S NEAR $x = 1$

The behaviors of pdf's near $x = 1$ are governed by the large-n limit of those moments.

5.1. The polarized case

The pdf's in LO are factorization-scheme independent. For large n, $\Delta q^\gamma_S(n)|_{\rm LO}$ and $\Delta q^\gamma_{NS}(n)|_{\rm LO}$ behave as $1/(n\ \ln\ n)$, while $\Delta G^\gamma(n)|_{\rm LO} \propto 1/(n\ \ln\ n)^2$. Thus in x space, the pdf's vanish for $x \to 1$. In fact we find

$$\begin{aligned}&\Delta q^\gamma_S(x)|_{\rm LO}\\ &\approx \frac{\alpha}{4\pi}\frac{4\pi}{\alpha_s(Q^2)}N_f\langle e^2\rangle\frac{9}{4}\ \frac{-1}{\ln\ (1-x)}\\ &\Delta G^\gamma(x)|_{\rm LO}\\ &\approx \frac{\alpha}{4\pi}\frac{4\pi}{\alpha_s(Q^2)}N_f\langle e^2\rangle\frac{1}{2}\ \frac{-\ln\ x}{\ln^2\ (1-x)}\ .\end{aligned} \tag{16}$$

The behaviors of $\Delta q^\gamma_{NS}(x)$ for $x \to 1$, both in LO and NLO, are always given by the corresponding expressions for $\Delta q^\gamma_S(x)$ with replacement of the charge factor $\langle e^2\rangle$ with $(\langle e^4\rangle - \langle e^2\rangle^2)$.

From analysis of the large n behaviors for the moments of the NLO pdf's in the $\overline{\rm MS}$ scheme, we find near $x = 1$,

$$\begin{aligned}\Delta q^\gamma_S(x)|_{\rm NLO,\overline{MS}} &\approx \frac{\alpha}{4\pi}N_f\langle e^2\rangle 6\ [-\ln(1-x)],\\ \Delta G^\gamma(x)|_{\rm NLO,\overline{MS}} &\approx \frac{\alpha}{4\pi}N_f\langle e^2\rangle 3\ [-\ln\ x]\ .\end{aligned} \tag{17}$$

It is remarkable that in the $\overline{\rm MS}$ scheme quark pdf's, $\Delta q^\gamma_S(x)|_{\rm NLO,\overline{MS}}$ and $\Delta q^\gamma_{NS}(x)|_{\rm NLO,\overline{MS}}$, diverge as $[-\ln(1-x)]$ for $x \to 1$. The NLO quark pdf's in the CI scheme also diverge as $x \to 1$. In fact we observe that $\Delta q^\gamma_S(x)|_{\rm NLO,CI}$ approaches $\Delta q^\gamma_S(x)|_{\rm NLO,\overline{MS}}$ for large x.

On the other hand, the OS scheme gives quite different behaviors near $x = 1$ for the quark pdf's. We find that, in x space, $\Delta q^\gamma_S(x)|_{\rm NLO,OS}$ does not diverge for $x \to 1$ but approaches a constant value:

$$\Delta q^\gamma_S(x)|_{\rm NLO,OS} \ \to\ \frac{\alpha}{4\pi}N_f\langle e^2\rangle\Big[\frac{69}{8}+\frac{3}{4}N_f\Big]. \tag{18}$$

5.2. The unpolarized case

In LO the pdf's of unpolarized virtual photon target have the same behaviors as the polarized case for $x \to 1$. We obtain

$$\begin{aligned}q^\gamma_S(x)|_{\rm LO} &\approx \Delta q^\gamma_S(x)|_{\rm LO}\\ G^\gamma(x)|_{\rm LO} &\approx \Delta G^\gamma(x)|_{\rm LO}\end{aligned} \tag{19}$$

Furthermore, we have found that the NLO behaviors of the pdf's, which are predicted by each factorization scheme for $x \to 1$, are the same both in the unpolarized and polarized cases. More specifically

$$\begin{aligned}q^\gamma_S(x)|_{{\rm NLO},\ a} &\approx \Delta q^\gamma_S(x)|_{{\rm NLO},\ a}\\ G^\gamma(x)|_{{\rm NLO},\ a} &\approx \Delta G^\gamma(x)|_{{\rm NLO},\ a}\end{aligned} \tag{20}$$

where $a = \overline{\rm MS},\ \ {\rm OS}$.

In DIS$_\gamma$ scheme, quark pdf's becomes negative and divergent for $x \to 1$. In fact, we find

$$q^\gamma_S(x)|_{\rm NLO,DIS_\gamma} \approx \frac{\alpha}{4\pi}\ 6N_f\langle e^2\rangle[\ln\ (1-x)] \tag{21}$$

This is due to the fact that the photonic coefficient function $C^\gamma_\gamma(x)$, which becomes negative and divergent for $x \to 1$ in $\overline{\rm MS}$, is absorbed into the quark pdf's in the DIS$_\gamma$ scheme.

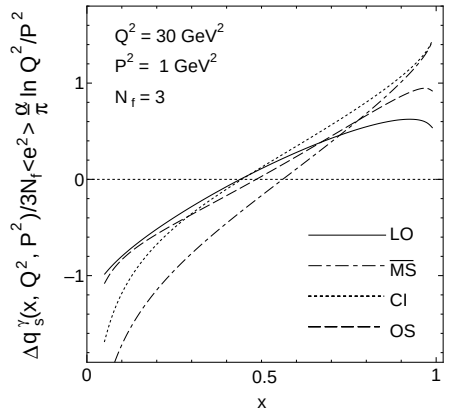

Figure 2. The polarized singlet quark distribution $\Delta q_S^\gamma(x, Q^2, P^2)$ in LO (solid line) and beyond LO. The NLO results are from $\overline{\rm MS}$(dash-dotted line), CI (short-dashed line), and OS (long-dashed line) schemes.

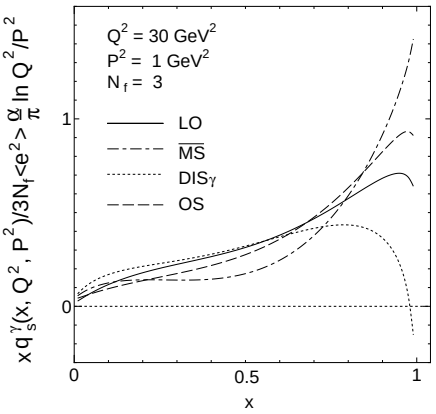

Figure 3. The unpolarized singlet quark distribution $xq_S^\gamma(x, Q^2, P^2)$ in LO (solid line) and beyond LO. The NLO results are from $\overline{\rm MS}$(dash-dotted line), OS (long-dashed line), and DIS$_\gamma$(short-dashed line) schemes.

6. NUMERICAL ANALYSIS

The pdf's are recovered from the moments by the inverse Mellin transformation. In Fig.2 we plot the singlet quark pdf $\Delta q_S^\gamma(x, Q^2, P^2)$ of polarized virtual photon both in LO and NLO in units of $(3N_f\langle e^2\rangle\alpha/\pi)\,\ln(Q^2/P^2)$. We have taken $N_f = 3$, $Q^2 = 30$ GeV^2, $P^2 = 1$ GeV^2, and the QCD scale parameter $\Lambda = 0.2$ GeV. We present the NLO results in three different factorization schemes, i.e., $\overline{\rm MS}$, CI and OS. The CI and OS lines cross the x-axis nearly at the same point, just below $x = 0.5$, while the $\overline{\rm MS}$ line crosses at above $x = 0.5$. This is understandable since we saw from Eq.(13) that the first moment of Δq_S^γ vanishes in the CI and OS schemes, while it is negative in the $\overline{\rm MS}$ scheme. As $x \to 1$, we observe that the $\overline{\rm MS}$ and CI lines continue to increase and actually tend to merge, while the OS line starts to drop. These behaviors are inferred from Eqs.(17-18). It is noted that the $\overline{\rm MS}$ line is much different from the LO one. We see that OS scheme predicts a better behavour for Δq_S^γ than other schemes in the sence that the OS line is closer to the LO one and does not diverge as $x \to 1$.

Concerning the non-singlet quark distribution $\Delta q_{NS}^\gamma(x, Q^2, P^2)$, we find that when we take into account the charge factors, it falls on the singlet quark distribution in almost all x region; namely two "normalized" distributions $\Delta\widetilde{q}_S^\gamma \equiv \Delta q_S^\gamma/\langle e^2\rangle$ and $\Delta\widetilde{q}_{NS}^\gamma \equiv \Delta q_{NS}^\gamma/(\langle e^4\rangle - \langle e^2\rangle^2)$ mostly overlap except at very small x region. Finally, compared with quark pdf's, the gluon distribution $\Delta G^\gamma(x, Q^2, P^2)$ is very much small in absolute value except at the small x region.

In Fig.3 we plot the singlet quark pdf $xq_S^\gamma(x, Q^2, P^2)$ inside unpolarized virtual photon target both in LO and NLO in units of $(3N_f\langle e^2\rangle\alpha/\pi)\,\ln(Q^2/P^2)$. Again we have taken $N_f = 3$, $Q^2 = 30$ GeV^2, $P^2 = 1$ GeV^2, and the QCD scale parameter $\Lambda = 0.2$ GeV. We present the NLO results in three different factorization schemes, i.e., $\overline{\rm MS}$, OS and DIS$_\gamma$. As in the polarized case, the $\overline{\rm MS}$ line deviates from the LO one, and diverges as $x \to 1$. The DIS$_\gamma$ line is close

to the LO line below $x < 0.7$, but negatively diverges as $x \to 1$. Again, in the unpolarized case, the OS scheme gives a better behavior for xq_S^γ. Actually, the OS line is closer to the LO one and starts to drop to reach the finite value for $x \to 1$.

7. SUMMARY

The behaviors of the pdf's inside the virtual photon target, polarized and unpolarized, can be predicted entirely up to NLO, but they are factorization-scheme-dependent. We have studied the scheme dependence of the pdf's in the virtual photon. In the case of polarized pdf's, the scheme dependence is clearly seen in the first moments and the large-x behaviors of quark distributions. In the umpolarized case, the scheme dependence is also observed in the large-x behaviors of quark distributions. The NLO quark pdf's predicted by the $\overline{\rm MS}$ scheme deviate substantially from the LO results and diverge as $x \to 1$, for both polarized and unpolarized cases. On the other hand, the OS scheme gives better behaviors for the quark pdf's in the sence that they are close to the LO pdf's and remain finite as $x \to 1$.

REFERENCES

1. T. Uematsu and T. F. Walsh, Nucl. Phys. **B199** (1982) 93.
2. K. Sasaki and T. Uematsu, Phys. Rev. **D59** (1999) 114011; Nucl. Phys. B (Proc. Suppl.) **79** (1999) 614.
3. W. Furmanski and R. Petronzio, Z. Phys. **C11** (1982) 293.
4. K. Sasaki and T. Uematsu, Phys. Lett. **B473** (2000) 309.
5. R. Mertig and W. L. van Neerven, Z. Phys. **C70** (1996) 637.
6. W. Vogelsang, Phys. Rev. **D54** (1996) 2023; Nucl. Phys. **B475** (1996) 47.
7. G. T. Bodwin and J. Qiu, Phys. Rev. **D41** (1990) 2755.
8. H.-Y. Cheng, Int. J. Mod. Phys. **A11** (1996) 5109; Phys. Lett. **B427** (1998) 371.
9. D. Müller and O. V. Teryaev, Phys. Rev. **D56** (1997) 2607.
10. R. D. Ball, S. Forte and G. Ridolfi, Phys. Lett. **B378** (1996) 255.
11. J. Kodaira, S. Matsuda, K. Sasaki and T. Uematsu, Nucl. Phys. **B159** (1979) 99.
12. J. Kodaira, Nucl. Phys.**B165** (1980) 129.
13. M. Glück, E. Reya and A .Vogt, Phys. Rev. **D45** (1992) 3986.
14. K. Sasaki and T. Uematsu, in preparation.